

LA-5048

C.3

CIC-14 REPORT COLLECTION  
**REPRODUCTION  
COPY**

Gamma-Ray Production Cross Sections for  
1- and 2-MeV Neutron Interactions with  
 $^{235}\text{U}$  and  $^{239}\text{Pu}$



**los alamos**  
**scientific laboratory**  
of the University of California  
LOS ALAMOS, NEW MEXICO 87544

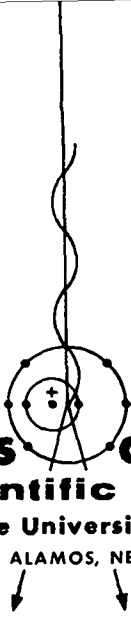
This report was prepared as an account of work sponsored by the United States Government. Neither the United States nor the United States Atomic Energy Commission, nor any of their employees, nor any of their contractors, subcontractors, or their employees, makes any warranty, express or implied, or assumes any legal liability or responsibility for the accuracy, completeness or usefulness of any information, apparatus, product or process disclosed, or represents that its use would not infringe privately owned rights.

Printed in the United States of America. Available from  
National Technical Information Service  
U. S. Department of Commerce  
5285 Port Royal Road  
Springfield, Virginia 22151  
Price: Printed Copy \$3.00; Microfiche \$0.95

LA-5048

UC-34

ISSUED: December 1972



**los alamos**  
**scientific laboratory**  
of the University of California  
LOS ALAMOS, NEW MEXICO 87544

Gamma-Ray Production Cross Sections for  
1- and 2-MeV Neutron Interactions with  
 $^{235}\text{U}$  and  $^{239}\text{Pu}$

by

D. M. Drake



GAMMA-RAY PRODUCTION CROSS SECTIONS FOR 1- AND 2-MeV  
NEUTRON INTERACTIONS WITH  $^{235}\text{U}$  AND  $^{239}\text{Pu}$

by  
D. M. Drake

ABSTRACT

Gamma-ray spectra have been measured for 1- and 2-MeV neutron interactions with  $^{235}\text{U}$  and  $^{239}\text{Pu}$  using a time-of-flight technique and an anti-Compton spectrometer. Gamma-ray production cross sections are determined and compared with previous measurements.

I. INTRODUCTION

A pulsed beam of neutrons from the Los Alamos Scientific Laboratory's (LASL) vertical Van de Graaff accelerator was used to bombard samples of  $^{235}\text{U}$  and  $^{239}\text{Pu}$  at neutron energies of 1 and 2 MeV. Prompt gamma-ray spectra were measured at  $45^\circ$  to the neutron beam with a NaI anti-Compton spectrometer. Two auxiliary measurements, neutron flux and spectrometer efficiency, are necessary to compute cross sections from the spectral data. The neutron flux was measured with a proton recoil telescope and a low-geometry fission counter. The spectrometer efficiency as a function of gamma-ray energy was measured with calibrated sources. Cross sections deduced from this experiment are compared with earlier data and the amount of energy emitted in the form of gamma rays is discussed.

II. EXPERIMENTAL ARRANGEMENTS

Figure 1 is a schematic diagram of the experimental arrangement. Protons, accelerated to appropriate energies by the LASL vertical Van de Graaff, came from the accelerator in bursts 10 nsec wide, with a repetition rate of 2 MHz. These bursts were subsequently compressed to 1 nsec by a Mobley bunching system.<sup>1</sup> A capacitive pickup provided a fiducial time signal that was used to separate neutrons from gamma rays by time of flight.

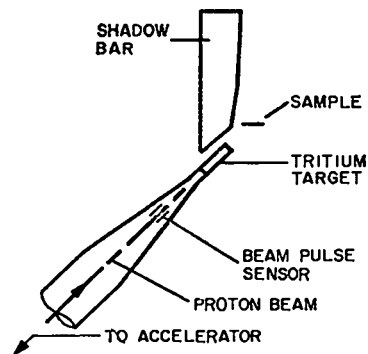
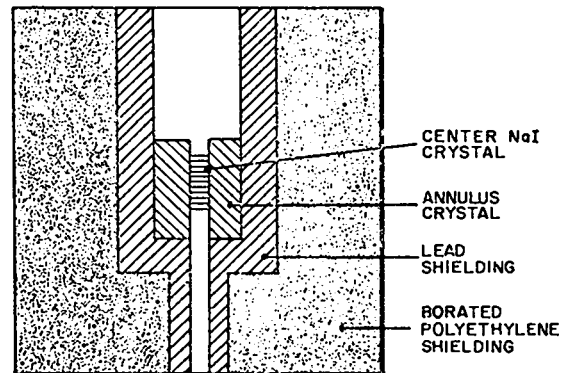


Fig. 1. Experimental arrangement.

The neutrons are produced by the  $t(p,n) {}^3\text{He}$  reaction in a 3.2-cm-long gas cell filled with tritium to a pressure of 2 atm. The molybdenum entrance foil of the gas cell was  $5.3\text{-mg/cm}^2$  thick.

Table I shows the energy loss in the gas and the straggling through the entrance foil for the incoming protons in this experiment. The spread in neutron energy is approximately equal to the sum of the straggling and energy loss of the protons in the gas.

TABLE I

ENERGETICS OF THE NEUTRON-PRODUCING PROTON BEAM

Neutron Energy (MeV)	Proton Energy (MeV)	Energy Lost in Foil (keV)	Straggling through Foil (keV)	Energy Lost in Gas (keV)
2	3.143	277	52	160
1	2.270	354	53	224

The four samples used in this experiment are described in Table II. The iron sample was used to check the consistency of the data over the course of the experiment. It was relatively simple to sum the number of counts in the 0.84-MeV gamma-ray peak produced by  ${}^{56}\text{Fe}(n,n'\gamma){}^{56}\text{Fe}$  to compare with previous runs. The plutonium sample was enclosed in a thin nickel can. A similar, but empty, nickel can was used as a background measurement for plutonium runs. The samples were placed about 10 cm from the neutron source. The axis of the cylindrical samples was collinear with the center line of the collimator. The spectrometer was located at an angle of  $45^\circ$  to the beam direction.

TABLE II

SAMPLE CHARACTERISTICS

Sample	Thickness (cm)	Diameter (cm)	Main Impurities	Weight (g)
${}^{235}\text{U}$	0.16	4.41	${}^{238}\text{U}$ (2.5 g)	46.9
${}^{238}\text{U}$	0.16	4.4		44.2
${}^{239}\text{Pu}$	0.16	4.1	Ga (0.3 g) ${}^{240}\text{Pu}$ (2.0 g)	32.7
Fe	0.16	4.4		18.8

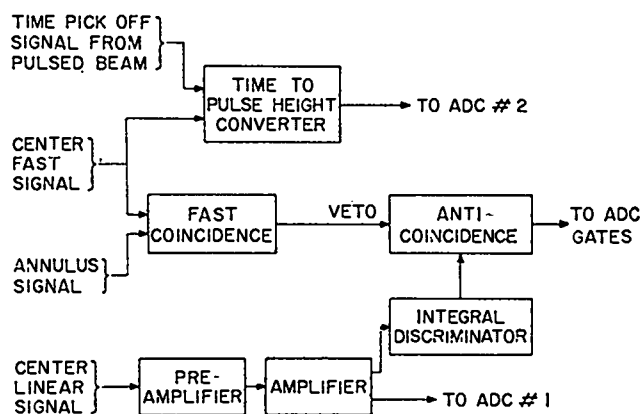


Fig. 2. Simplified diagram of the electronic system.

The spectrometer used in this experiment consisted of two sodium iodide crystals, one of which (25-cm diam by 30-cm long) had an annular shape and nearly surrounded the second or central detector (5.7-cm diam by 15.2-cm long). These crystals were placed in the center of a large shield-collimator made of borated polyethylene and lead. The collimator aperture was 5 cm in diameter.

The essential parts of the electronic system are shown in Fig. 2. Because the anticoincidence circuit used here had a rather large dead time, a fast coincidence between the center and annulus crystals was required before the anticoincidence was activated. This fast coincidence provides considerably faster data collection than would be possible if all the annulus pulses were used to activate the anticoincidence system.

III. DATA COLLECTION

A. Timing

A fast pulse from the anode of the center photomultiplier was used to start a time-to-amplitude converter, and a pulse derived from the beam pickoff was used as a stop pulse. Figure 3 shows a time-of-flight spectrum for 1-MeV bombardment of the  ${}^{235}\text{U}$  sample. Time-of-flight spectra for the other samples are similar. To aid in the data analysis, the time spectra were divided into three regions and pulse height data were recorded corresponding to each of these intervals. The three intervals

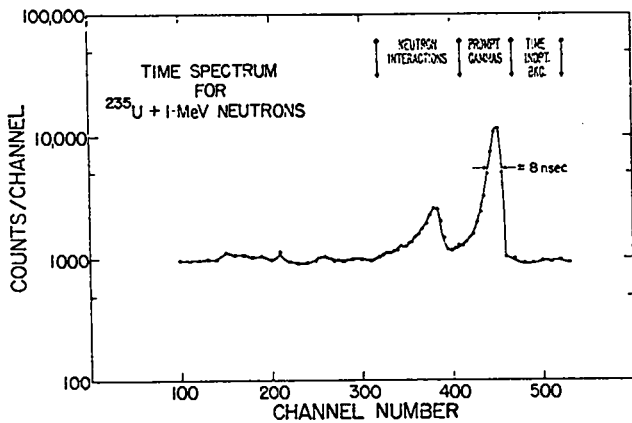


Fig. 3. Time-of-flight spectrum. The time spectrum is divided into three intervals which represent time-independent background, prompt gamma rays, and neutron interactions in the crystal.

shown in Fig. 3 are labeled 1) time-independent background, 2) prompt gamma rays (gamma rays emitted within 40 nsec of the neutron burst), and 3) neutron interactions. The time-independent part of the spectrum records events that occur nearly 500 nsec after a burst of neutrons is produced. It is supposed to measure a type of background, underlying the whole time spectrum, that varies slowly, such as pulses from radioactivity and neutrons that have been scattered in the room several times. The prompt gamma-ray peak corresponds to gamma rays that are made in the sample by a burst of neutrons. The third interval records the pulse height spectrum from the neutrons scattered in the crystal.

### B. Pulse Height Spectra

Pulse height spectra for the above intervals, as well as the time-of-flight spectrum for each run, were recorded on magnetic tape. Figures 4 through 7 show prompt pulse height spectra for  $^{235}\text{U}$  and  $^{239}\text{Pu}$  for incident neutron energies of 1 and 2 MeV. These figures also show the time-independent background pulse height spectra for the lower pulse heights. Figure 6, the 2-MeV neutron bombardment of  $^{235}\text{U}$ , shows a very intense gamma ray at 0.185 MeV in both the prompt gamma-ray interval and the time-independent background. A Ge(Li) detector was used to look at this peak away from the neutron beam and it appeared

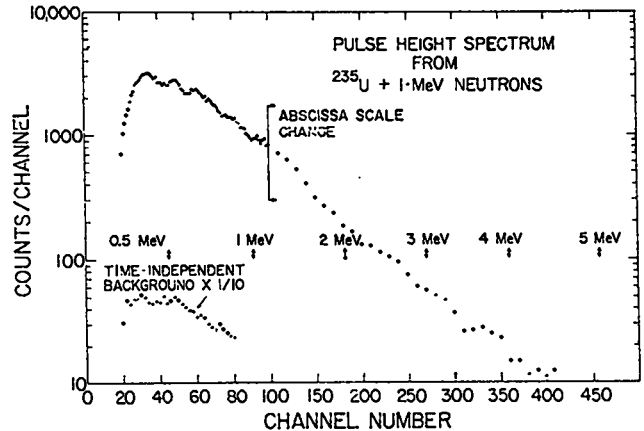


Fig. 4. Pulse height spectrum for prompt gamma rays from  $^{235}\text{U}$  + 1-MeV neutrons.

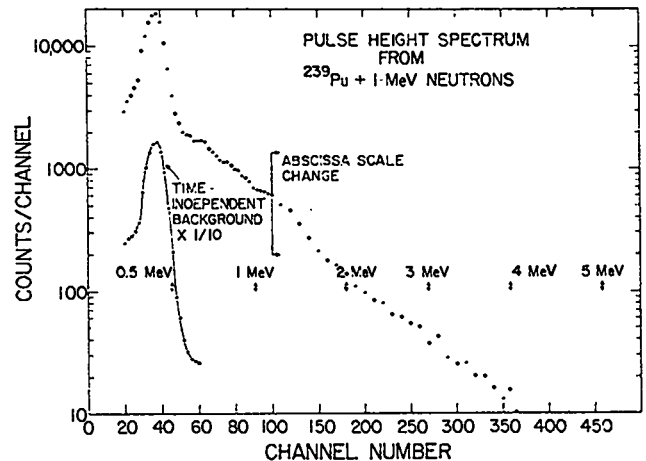


Fig. 5. Pulse height spectrum for prompt gamma rays from  $^{239}\text{Pu}$  + 1-MeV neutrons.

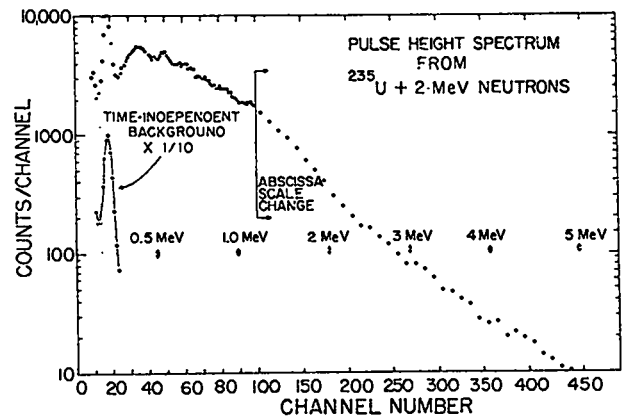


Fig. 6. Pulse height spectrum for prompt gamma rays from  $^{235}\text{U}$  + 2-MeV neutrons.

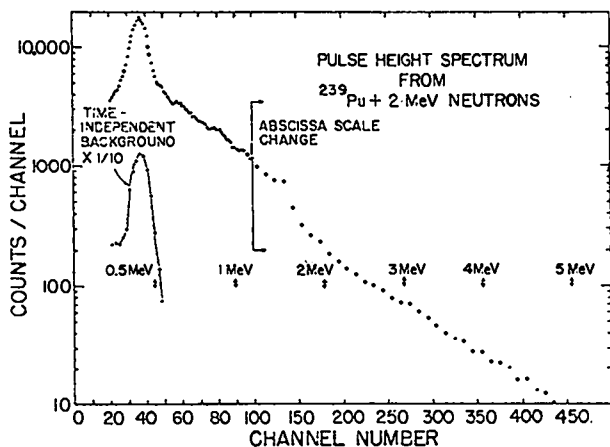


Fig. 7. Pulse height spectrum for prompt gamma rays from  $^{239}\text{Pu} + 2\text{-MeV}$  neutrons.

to be a single line, probably the 0.185-MeV gamma ray present in the decay of  $^{235}\text{U}$ . This peak did not show up in the 1-MeV spectrum because the bias was set to eliminate it.

A similar peak appears in the  $^{239}\text{Pu}$  spectra near 400 keV. This peak is made up of several gamma rays and is similarly due to the radioactivity of the plutonium sample. A Ge(Li) spectrum of these gamma rays shows intense lines at 0.43, 0.39, and 0.22 MeV, with less intense lines at 0.41, 0.36, and 0.34 MeV. Because the pulses from these lines are several times more intense than the pulses from neutron interactions in the sample, a small uncertainty in background subtraction could lead to a rather large uncertainty in the net spectrum for this region.

### C. Energy Scale

The energy scale was measured periodically with gamma-ray sources and was quite stable during a series of runs. In addition, pulse height spectra corresponding to times when fast neutrons hit the crystal showed characteristic gamma rays resulting from neutron inelastic scattering in the sodium iodide crystal. Because the gamma-ray spectra from both plutonium and uranium have little structure, the pulse height spectrum for the neutron interactions in the crystal (see Fig. 8), together with the sample activity, was useful for checking gain stability.

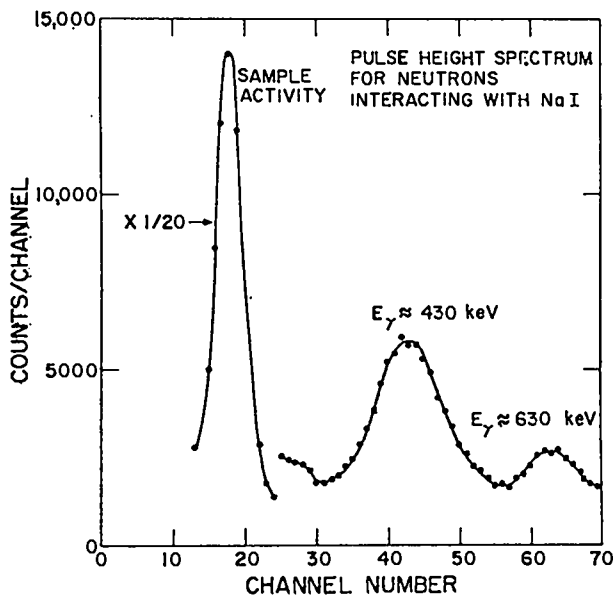


Fig. 8. Pulse height spectrum for the time interval corresponding to neutron interactions in the sodium iodide crystal.

## IV. ANALYSIS

To compute cross sections, the net prompt gamma-ray pulse height spectrum must be transformed or unfolded to a gamma-ray spectrum by using response functions that are appropriate for the spectrometer. One must also measure the neutron flux that strikes the sample, as well as the detection efficiency of the gamma-ray spectrometer as a function of energy.

### A. Unfolding

The data reported here were stripped primarily by hand using the response shapes obtained from the same gamma-ray sources that were used in determining the efficiency. Some of the spectra were also unfolded using a computer code, LSMUN.<sup>2</sup>

Comparison of the results of the computer unfold with the hand-stripping technique showed only minor (less than 3%) differences. The good agreement for these two unfolding methods probably is due to the shape of the spectra which rise steeply as one goes from high to low energy. The tails of the high-energy gamma rays account for only about 12% of the counts in any of the lower energy intervals.

### B. Detector Efficiency

The efficiency of the detector was measured from 0.28 to 1.84 MeV with two different sets of gamma-ray sources obtained from the International Atomic Energy Agency (IAEA). Efficiencies at higher energies were measured using  $^{24}\text{Na}$  at 2.75 MeV, PuBe at 4.4 MeV, and an encapsulated mixture of  $^{13}\text{C}$  and  $^{244}\text{Cm}$  borrowed from Oak Ridge National Laboratory (ORNL)<sup>3</sup> as a source of 6.13-MeV gamma rays. The efficiency curve is shown in Fig. 9. The points represent the ratio of the number of counts in the full energy peak to the number of gamma rays emitted from the source. The distance from the source to the detector for this calibration curve was 87 cm. The same distance was used for sample-to-detector in the experiment.

### C. Flux Measurements

The neutron flux at 2 MeV was measured with a proton recoil telescope and a low-geometry fission detector. The fission detector consisted of a thin-walled cylindrical aluminum can with a  $^{235}\text{U}$  foil,  $0.5\text{-mg/cm}^2$  thick, mounted on one end and a silicon detector on the other. The foil thickness was determined by alpha-particle counting in a standard geometry. After the foil was mounted in the neutron detector, another alpha count was made. This second count was used to determine the effective solid angle of the silicon counter. A calculation of the solid angle using the measured dimensions of the detector agreed to about 1% with the solid angle determined by alpha-particle counting.

Corrections applied to the flux determined by the fission detector measurements were 4% for in-scattering by the material of the fission counter, 1% for room-scattered neutrons, and 1.5% for the center-of-mass motion, assuming isotropic fragment distribution in the center-of-mass system.

The proton recoil telescope contained a polyethylene foil approximately  $1\text{ mg/cm}^2$  thick located 7.5 cm in front of a collimated silicon detector. The small-angle formula<sup>4</sup> was used to determine the efficiency of this counter. A correction of 1% was made for attenuation of the neutrons by the entrance window.

The fluxes measured with the telescope and the fission counter at 2 MeV agreed within 2%. The standard deviation for the number of counts in the

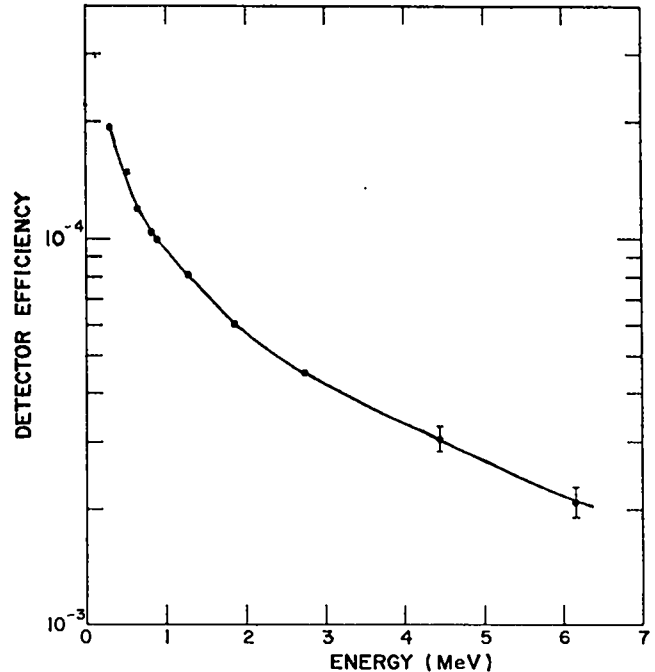


Fig. 9. Efficiency curve for the gamma spectrometer. The ordinate represents the number of counts in the full energy peak divided by the number of gamma rays emitted by the source.

fission measurement was 1.5% and was less than 0.5% for the measurement done with the proton recoil telescope.

Neutron flux at 1.0-MeV neutron energy was measured only with the fission counter, and corrections similar to those described above were applied. This 1-MeV flux agrees with the value obtained by multiplying the flux at 2 MeV by the appropriate ratios of current integrator values, gas cell pressures, and  $T(p,n)^3\text{He}$  cross sections.

### D. Cross Section Calculation

The cross sections were computed using the formula

$$\sigma(\theta, E_\gamma) = \frac{G d^2}{4\pi N \epsilon Q F} \quad (1)$$

where  $G$  is the number of unfolded gamma-ray counts per million electron volt,  $d$  is the average distance from the neutron source to the sample,  $N$  is the number of atoms in the sample,  $\epsilon$  is the gamma-ray detection efficiency,  $Q$  is the number of

microcoulombs collected during the run, and F is the neutron flux in neutrons/steradian-microcoulomb.

#### E. Corrections

The formula of Eq. (1) needs some corrections, most of which are a few percent in magnitude.

A gallium phosphide light-emitting diode, positioned in a thin light pipe connecting the center crystal and its photomultiplier, was pulsed about 10 times/sec. The light output from this diode could be varied by changing the size of the pulse, and in this experiment the light output was equivalent to a gamma ray of about 13 MeV, an energy well above any gamma rays of interest here. The live time of the whole electronic system, if the accelerator beam is reasonably steady, is given by the ratio of the number of pulses recorded in the spectra to the number of times the diode fired during a run. Thus the experimenter does not have to know the dead-time characteristics of individual components of the system. In this experiment, the dead-time corrections were about 5% for the  $^{239}\text{Pu}$  runs and 3% for the  $^{235}\text{U}$  runs.

Gamma-ray attenuation in the sample was computed using gamma-ray cross sections from the tables of Storm and Israel.<sup>5</sup> The correction went from 6% at 5-MeV to 10% at 1-MeV gamma-ray energy. Below 1 MeV the correction increased steeply to 47% at 300 keV.

Interactions of the neutrons with the nuclei in the sample have an effect that can be treated as a flux increase. Elastic and inelastic scattering increase the average path length of the neutrons through the sample and each fission event produces  $\bar{\nu}$  neutrons. These processes are computed to be equivalent to an increase in the flux by 8% in  $^{235}\text{U}$  and 9% in  $^{239}\text{Pu}$ .

A sample of  $^{238}\text{U}$  with the same dimensions as the  $^{235}\text{U}$  sample was also bombarded with 1- and 2-MeV neutrons during this experiment to correct for the 5% of  $^{238}\text{U}$  in the  $^{235}\text{U}$  sample. No correction was made for the 6%  $^{240}\text{Pu}$  in the plutonium sample, because  $^{240}\text{Pu}$  and  $^{239}\text{Pu}$  cross sections are so similar that only negligible errors are introduced if they are treated alike.

#### V. ESTIMATE OF UNCERTAINTIES

The experiment should have an uncertainty in gamma-ray production cross section of 13% at 6-MeV, and about 9% at 1-MeV gamma-ray energy. Uncertainty in the total energy per fission emitted in gamma rays is about 6%.

Uncertainties in the efficiency of the detector vary with gamma-ray energy. The 6.13-MeV source strength was known to about 10%, the 4.4-MeV source strength to about 7%. The other sources were all known to an accuracy better than 2%.

Neutron flux measurements made with the low-geometry fission detector agreed with the proton recoil telescope measurement within 2% after corrections of 6% were applied to the fission detector, and 1% to the telescope. Because the flux measurements are based primarily on fission cross sections, the flux uncertainty is at least as large as that of the fission cross section ( $\approx 5\%$ ) and is taken to be 6%.

Errors made in unfolding the spectra are rather uncertain. The hand unfold agrees generally within 3% of that done by computer. An upper limit on the error introduced by the unfolding process is 5%. If the spectra are not unfolded at all, i.e., no tail on the gamma-ray response functions, the computed cross sections increase by about 12% over the measured gamma-ray energy range.

#### VI. DISCUSSION

Gamma rays produced by 1- to 2-MeV neutron bombardment of  $^{235}\text{U}$  and  $^{239}\text{Pu}$  come primarily from radiative capture, inelastic scattering, and de-excitation of fission fragments. This discussion focuses on two aspects of these gamma rays: the total energy emitted in the form of gamma rays, and the cross section as a function of gamma-ray energy.

##### A. Energy Emitted as Prompt Gamma Rays

The total energy emitted in the form of gamma rays is one quantity that can be compared with the energy that would be expected from the various reactions that occur when neutrons interact with fissionable nuclei. Only the three reactions mentioned above are considered.

For each capture event, the amount of gamma-ray energy emitted is equal to the sum of the binding energy of a neutron in  $^{236}\text{U}$  or  $^{240}\text{Pu}$  (about 6.4 MeV

for each) and the kinetic energy of the incident neutron (center-of-mass energy is neglected).

The gamma-ray energy emitted in an inelastic scattering event is equal to the difference in kinetic energy of the incident and scattered neutron. If one assumes a compound nucleus model for the scattering, the average energy of the scattered neutron is  $2T$  for an evaporation spectrum, where  $T$  is the nuclear temperature. The gamma-ray energy for an inelastic event can therefore be written  $E_{\gamma i} = (E_n - 2T)$ .

The gamma-ray energy emitted by deexcitation of the fission fragments should be about the same as that for thermal fission which has been measured at 6.51 (Ref. 6) and 7.2 MeV (Ref. 7) for  $^{235}\text{U}$  and 6.8 MeV (Ref. 6) for  $^{239}\text{Pu}$  for gamma-ray energies from 0.15 to 10 MeV.

We add the average energy emitted in the form of gamma rays for each of these three processes, weighted by the probability per nonelastic event that that particular reaction occurs, and obtain the average energy emitted as gamma rays per nonelastic event.

$$\bar{E}_{\gamma n} = \frac{\sigma_i}{\sigma_n} (E_n - 2T) + \frac{\sigma_c}{\sigma_n} (Q + E_n) + \frac{\sigma_f}{\sigma_n} E_f \quad (2)$$

Here  $\sigma_n$  = nonelastic cross section,  $\sigma_i$  = inelastic scattering cross section,  $\sigma_c$  = capture cross section,  $\sigma_f$  = fission cross section,  $E_f$  = gamma-ray energy emitted in thermal fission,  $Q$  is the binding energy of the target nucleus plus neutron, and  $E_n$  is the kinetic energy of the neutron.

Similarly, the average energy per fission event emitted by all processes as gamma rays is given by

$$\bar{E}_{\gamma f} = \frac{\sigma_i}{\sigma_f} (E_n - 2T) + \frac{\sigma_c}{\sigma_f} (Q + E_n) + E_f \quad (3)$$

This is a reasonable quantity with which to compare the experimental results. To the first order the measurement of  $\bar{E}_{\gamma f}$  is independent of the fission cross section, because the fission cross section enters into the flux measurements and the calculation of the number of fissions in the sample in a similar way.

Table III shows our experimental results and estimates based on Eq. (3). Comparison of the last two columns shows that the experimental values agree fairly well with the expected yield of gamma-ray

TABLE III

COMPARISON OF EXPECTED TOTAL EMITTED GAMMA-RAY ENERGY WITH EXPERIMENTAL MEASUREMENTS

$E_n$ (MeV)	$\sigma_c^a$ (barns)	$\sigma_f^a$ (barns)	$\sigma_i^a$ (barns)	$T$ (MeV)	Expected Total Energy (MeV)	Experi- mental <sup>b</sup> Value (MeV)
<u><math>^{235}\text{U}</math></u>						
1.0+	0.11	1.23	1.37	0.18	7.9-8.6 <sup>c</sup>	8.4+0.5
2.0+	0.05	1.31	1.75	0.27	8.8-9.5	9.3+0.6
<u><math>^{239}\text{Pu}</math></u>						
1.0+	0.03	1.72	1.64	0.18	7.5	8.5
2.0+	0.01	2.06	1.96	0.27	8.2	8.5

<sup>a</sup>See Ref. 9.

<sup>b</sup>Experimental value is the measured value for  $0.25 < E_\gamma \leq 5.5$  MeV plus 0.25 MeV estimated from ORNL-4457 for gamma rays above 5.5 MeV and below 0.25 MeV.

<sup>c</sup>The range in "Expected Total Energy" is due to the difference in the GRT and ORNL measurements at thermal neutron energy.

energy. The experimental values listed in the last column of Table III are our measurement from 0.25 to 5.5 MeV, plus 0.25 MeV for gamma rays below 0.25 MeV and above 5.5 MeV, estimated from thermal fission data.<sup>7</sup>

The agreement between the last two columns in Table II is considerably improved if one takes account of the different time intervals used to define "prompt" gamma rays in this experiment and the two measurements done at thermal neutron energies.<sup>6,7</sup> The present measurement included gamma rays emitted up to 40 nsec after a neutron burst occurred; the estimate for  $^{239}\text{Pu}$  and the lower estimate for  $^{235}\text{U}$  are based on a time interval of 10 nsec, while the higher estimate for  $^{235}\text{U}$  included gamma rays up to  $\sim 80$  nsec after fission. A third measurement by Pleasonton<sup>8</sup> shows that the interval between 10 and 80 nsec after a fission event can account for about 1 MeV worth of gamma-ray energy.

Figure 10 compares the present results for 1-MeV neutrons on both  $^{235}\text{U}$  and  $^{239}\text{Pu}$  plotted as the average energy of gamma rays emitted per fission vs gamma energy. Also plotted are the data from Gulf Radiation Technology<sup>6</sup> (GRT) for thermal fission of  $^{235}\text{U}$  and  $^{239}\text{Pu}$  and from Oak Ridge National Laboratory<sup>7</sup> (ORNL) for thermal fission of  $^{235}\text{U}$ . The differences between

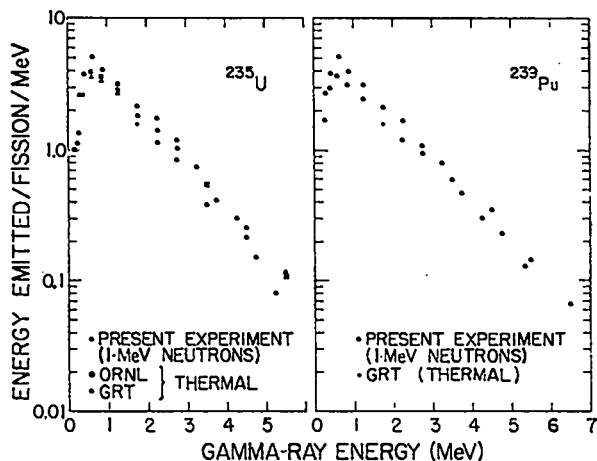


Fig. 10. Gamma-ray energy emitted per fission from  $^{235}\text{U}$  and  $^{239}\text{Pu}$ . Energy emitted per fission measured in the present experiment is compared to other measurements made with thermal neutron-induced fission.

our results and the thermal fission experiments are attributable to capture and inelastic scattering.

#### B. Cross Sections

Cross sections are listed in Table IV. Figures 11 through 14 display our results as well as some early results of Texas Nuclear Corporation.<sup>10</sup> In the places where the data overlap the agreement is very good. These cross sections have also been compared with the recent evaluations of Stewart and Hunter,<sup>11</sup> again with good agreement. The cross sections presented here show that the Stewart and Hunter treatment of energy dependence of the cross section at low gamma-ray energy is reasonable. Although the cross section is large at the lower gamma-ray energy (approximately 40% of the cross section is below  $E_\gamma = 0.5$  MeV), the amount of gamma-ray energy below 0.5 MeV is only about 10% of the total.

TABLE IV  
GAMMA-RAY PRODUCTION CROSS SECTIONS FOR  $^{235}\text{U}$   
AND  $^{239}\text{Pu}$  AT 1- AND 2-MeV NEUTRON ENERGY

Gamma Energy Interval (MeV)	$\sigma(\theta, E_\gamma)$ (mb/sr-MeV) at $45^\circ$			
	$^{239}\text{Pu}$		$^{235}\text{U}$	
	1 MeV	2 MeV	1 MeV	2 MeV
0.25-0.35	1320	1520	910	935
0.35-0.50	1278	1690	896	974
0.50-0.75	1140	1354	800	871
0.75-1.0	634	765	454	560
1.0-1.5	350	441	252	346
1.5-2.0	170	198	121	160
2.0-2.5	105	103	76.4	71.6
2.5-3.0	55	61	43.2	41.8
3.0-3.5	34.5	34.2	22.6	25.7
3.5-4.0	17.6	23.2	10.8	14.6
4.0-4.5	10.0	14.9	7.1	9.1
4.5-5.0	6.8	8.0	3.4	4.6
5.0-5.5	3.4	5.4	1.8	3.0

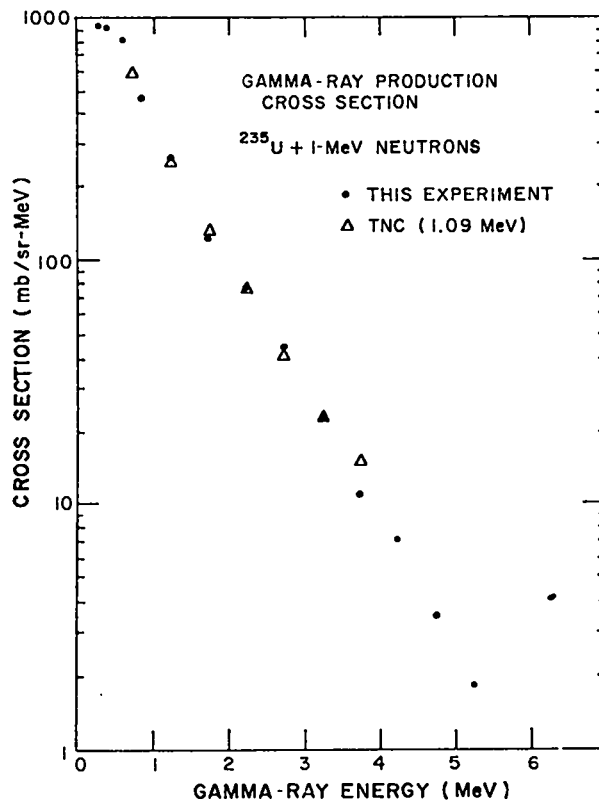


Fig. 11. Gamma-ray production cross section for  $^{235}\text{U} + 1\text{-MeV}$  neutrons.

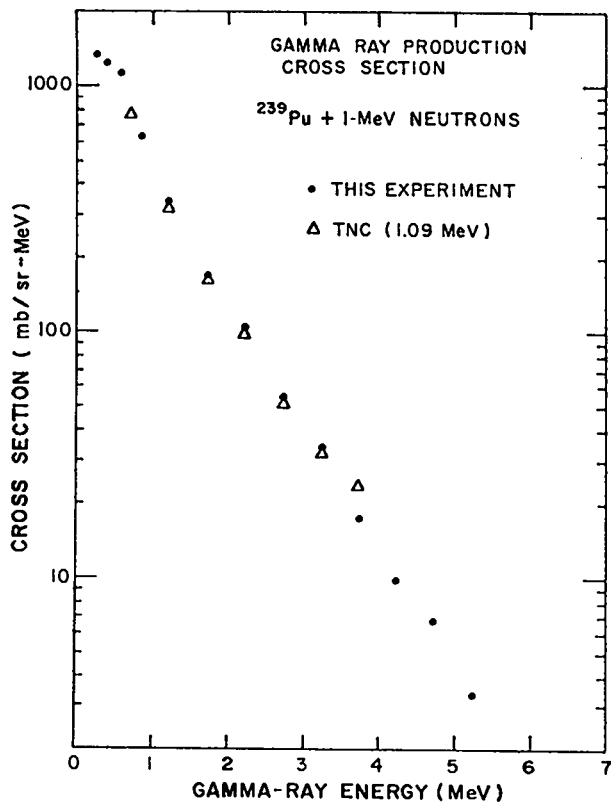


Fig. 12. Gamma-ray production cross section for  $^{239}\text{Pu} + 1\text{-MeV}$  neutrons.

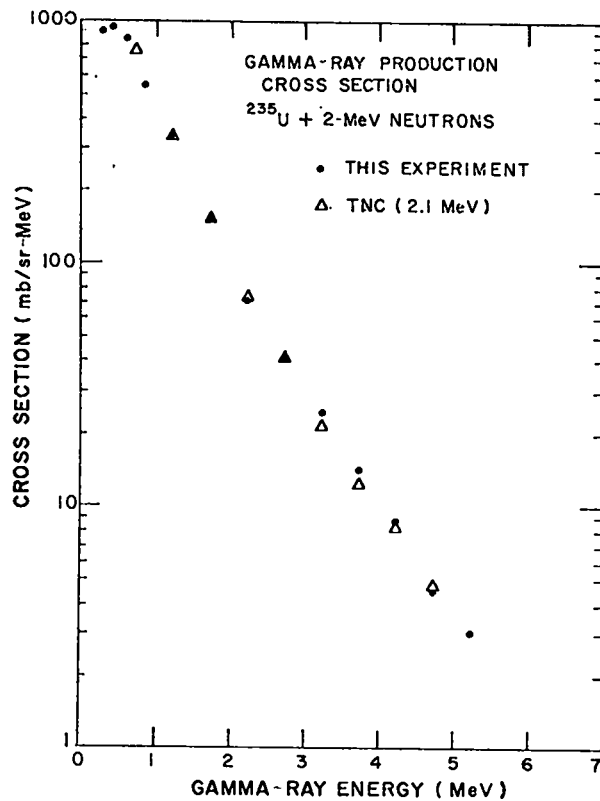


Fig. 13. Gamma-ray production cross section for  $^{235}\text{U} + 2\text{-MeV}$  neutrons.

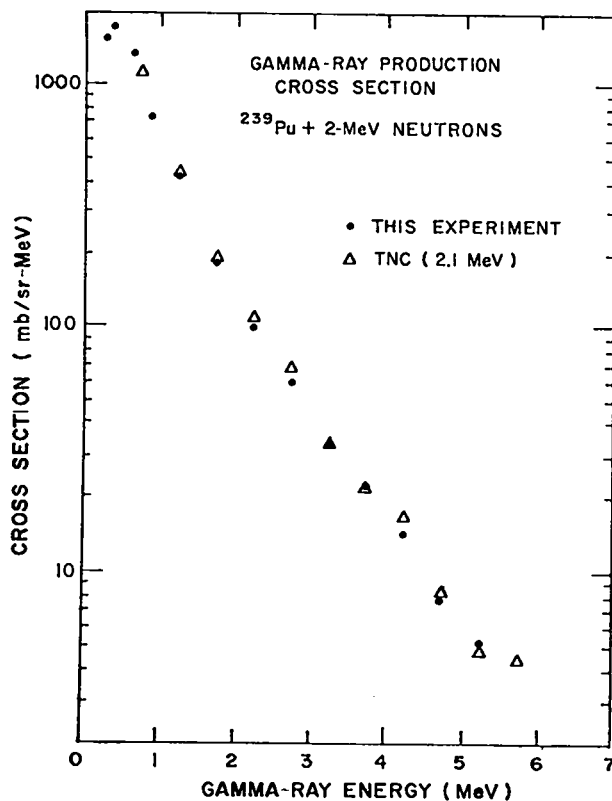


Fig. 14. Gamma-ray production cross section for  $^{239}\text{Pu} + 2\text{-MeV}$  neutrons.

REFERENCES

1. L. Cranberg, R. A. Fernald, F. S. Hahn, and E. F. Shrader, "Production of High Intensity Ion Pulses of Nanosecond Duration," Nucl. Instr. Meth. 12, 335-340 (1961).
2. C. S. Young, "Least Structure Techniques in Unfolding," Los Alamos Scientific Laboratory report LA-DC-12360 (February 1971).
3. J. K. Dickens and R. D. Baybarz, "A Monoenergetic 6130-keV Gamma-Ray Source for Detector Calibration," Oak Ridge National Laboratory report ORNL-TM-2958 (April 1970).
4. S. J. Bame, Jr., E. Haddad, J. E. Perry, Jr., and R. K. Smith, "Absolute Determination of Monoenergetic Neutron Flux in the Energy Range 1 to 30 MeV," Rev. Sci. Instr. 28, 997-1006 (1957).
5. E. Storm and H. Israel, "Photon Cross Sections from 0.001 to 100 MeV for Elements 1 through 100," Los Alamos Scientific Laboratory report LA-3753 (November 1967).
6. V. V. Verbinski and R. E. Sund, "Measurement of Prompt Gamma Rays from Thermal Neutron Fission of  $^{235}\text{U}$  and  $^{239}\text{Pu}$ , and from Spontaneous Fission of  $^{252}\text{Cf}$ . Annual Summary Report, May 15, 1967 through November 30, 1968," Gulf Radiation Technology, San Diego, report GA-9148 (April 1969).
7. R. W. Peele and F. C. Maienschein, "The Absolute Spectrum of Photons Emitted in Coincidence with Thermal-Neutron Fission of  $^{235}\text{U}$ ," Oak Ridge National Laboratory report ORNL-4457 (April 1970).
8. F. Pleasonton, R. L. Ferguson, and H. W. Schmitt, "Prompt Gamma Rays Emitted in the Thermal Neutron-Induced Fission of  $^{235}\text{U}$ ," Phys. Rev. C, Vol. 6, #3, 1023 (1972).
9. ENDF/B, Version III.
10. D. O. Nellis and I. L. Morgan, "Gamma Ray Production Cross Sections," Texas Nuclear Corporation report ORO-2791-17 (June 1966).
11. L. Stewart and R. E. Hunter, "Evaluated Neutron-Induced Gamma-Ray Production Cross Sections for  $^{235}\text{U}$  and  $^{238}\text{U}$ ," Los Alamos Scientific Laboratory report LA-4918 (July 1972); R. E. Hunter and L. Stewart, "Evaluated Neutron-Induced Gamma-Ray Production Cross Sections for  $^{239}\text{Pu}$  and  $^{240}\text{Pu}$ ," Los Alamos Scientific Laboratory report LA-4901 (July 1972).